International Journal of Robotics and Automation (IJRA)
Vol.8, No.4, December 2019, pp. 301~312
ISSN: 2089-4856, DOI: 10.11591/ijra.v8i4.pp301-312

Control shunt active filter based on *dq* frame using current model prediction

Chi Nguyen Van, Hoang Dang Danh
Thai Nguyen University of Technology, Vietnam

Article Info

Article history:

Received Apr 26, 2019
Revised Sep 20, 2019
Accepted Oct 6, 2019

Keywords:

Active power filter
CCVSI
Pi controller
Power quality
Total harmonic distortion

ABSTRACT

The nonlinear loads present more in the power systems in the practice today by developing of electronic technology and using the small distributed power sources (solar power, wind power etc.), this causes the increasing the high frequency switch devices etc. in the power network. Nonlinear loads cause non-sinusoidal currents and voltages with harmonic components, increasing the reactive power, overload of power lines and electrical devices, low power factor and affecting badly to the networks. Shunt active filters (SAF) with current controlled voltage source inverters (CCVSI) are used effectively to reduce the harmonics and to balance the phases sinusoidal source currents by generating the currents to compensate the harmonic currents caused by the nonlinear loads. In this paper we suppose a control strategy to generate the compensation currents of SAF by using the current model predictive engineering. This method is better than the control strategy using PI controller in term of transient time. The desired compensation currents can track exactly the reference compensation currents on the *dq* frame. The simulation results implemented on the nonlinear load, a full bridge rectifier and 3 phase unbalance load, show that the transient period decrease from 0.1s to 0.02s in comparing with PI controller. The experimental results proof that the THD of source currents decrease from 24.8% to 5.4% when using the proposed method.

Corresponding Author:

Chi Nguyen Van,
Department of Control Engineering and Instruments,
Thai Nguyen University of Technology,
3/2 street, Thai Nguyen City, Viet Nam.
Email: ngchi@tnut.edu.vn

1. INTRODUCTION

The developing quickly of the electrical engineering technology makes the power systems to be more complex in which the industrial, commercial loads and data center loads are increasing rapidly. The industrial loads include the motor driven by high frequency switch inverters, high frequency electrical furnaces, saturated motors, the commercial loads in the buildings are organized by saturated motors, HAVC load, LED, computers, data storage systems, special electronics devices, etc. All loads described as above are called by nonlinear loads and they are the causes generating some issues about the quality of the power systems [1]. Some of the major issues related to current harmonics include generator burnouts, vibration in motors while operating, computer network failures etc. To measure the harmonics distortion present, the index THD is used, THD is defined as the summation of all the harmonics components of the current waveform compared against the fundamental component of the current waveform. By the IEEE std. 519, the THD of the source current should be less than 5%.

To reduce the harmonics, owing to the advancement in power electronic switches the SAF is used widely nowadays. The SAF is connected in parallel with nonlinear load to compensate the higher order

harmonics currents based on CCVSI. The position in the power system and the typical structure of SAF is depicted respectively in the Figure 1a and 1b [2].

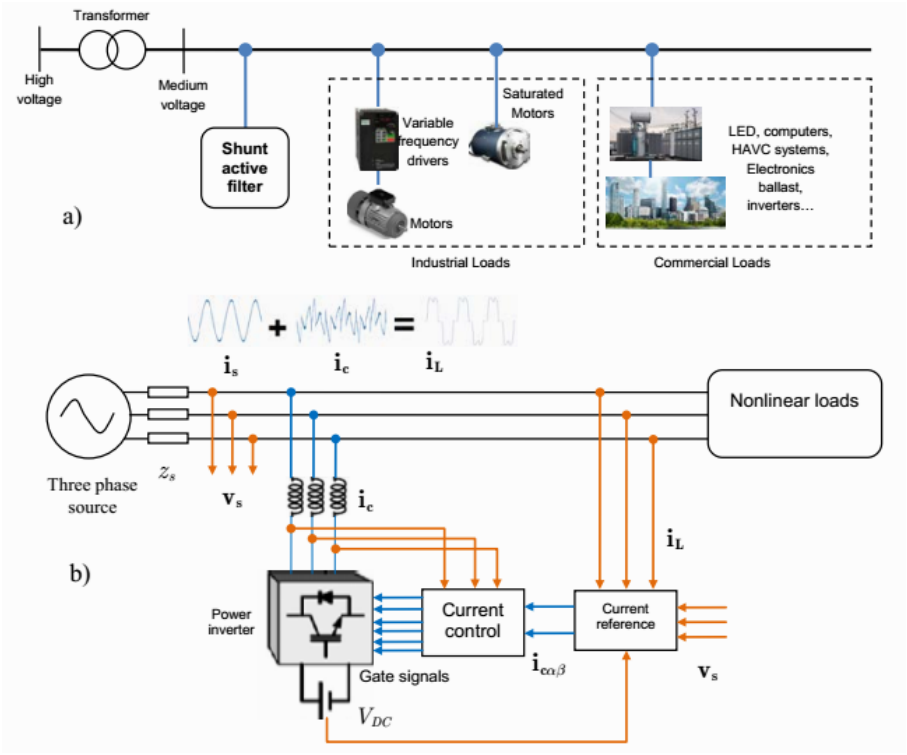

Figure 1. a) The position of SAF on the power system; b) The typical structure of SAF using the CCVSI

To implement the control outer loop, generating the desired compensation currents, we need the extra control loop, that determines the active power loss p_{loss} used to calculate the $\mathbf{i}_{\text{cref}}$. The active power loss normally is determined by PI controller in Oder to maintain the constant voltage DC across on the capacitor, it is shown in Figure 2. The transfer function of the plan for this extra control loop is as follows:

$$\mathrm{G}_{ex}(s) = \frac{k_{ex}}{\tau_{ex} s + 1} \tag{1}$$

where $k_{\text{ex}} = R / 2V_{co}, \tau_{\text{ex}} = 2 / RC$, R is the resistance parallel to the capacitor SAF, V_{co} is the reference capacitor voltage, C is the rated capacitance. The role of outer loop is to measure the load currents, source voltages, and then calculates the reactive power, reference active power that needs to be compensated. All calculations are implemented on the *dq* frame as described on the Figure 3.

Suppose that the load current distorted by harmonics $\mathbf{i}_{\text{L}}$, SAF measures the $\mathbf{i}_{\text{L}}$ and then calculates the compensation currents injecting to the power system $\mathbf{i}_{\text{C}}$ such that the source currents $\mathbf{i}_{\text{S}} = \mathbf{i}_{\text{L}} + \mathbf{i}_{\text{C}}$ maintain the sinusoidal waveform. It means that the harmonic currents caused by the nonlinear load are compensated completely by the compensation currents $\mathbf{i}_{\text{C}}$. The control strategy of SAF includes two control loop: the outer loop and the inner loop. The outer loop is used to calculate the reference compensation currents $\mathbf{i}_{\text{Cref}}$ based on the load currents measured $\mathbf{i}_{\text{L}}$, the inner loop makes the compensation current $\mathbf{i}_{\text{C}}$ tracking the reference currents by controlling the CCVSI using IGBT.

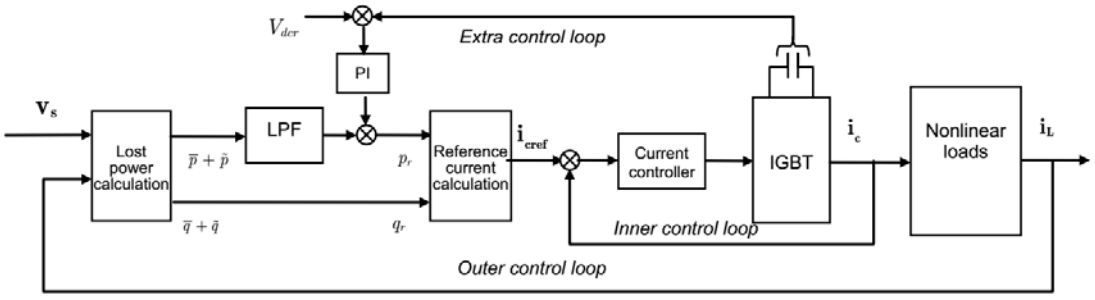

Figure 2. The structure of control loops of SAF

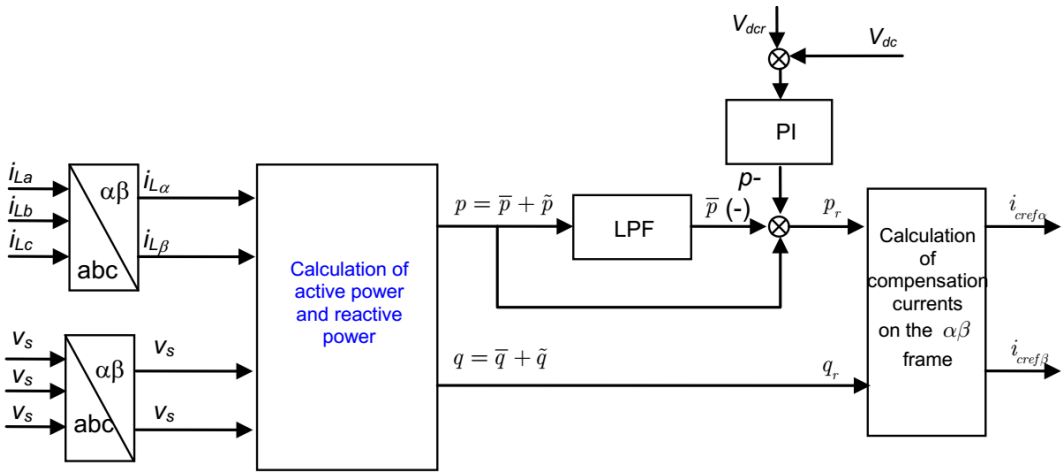

Figure 3. The structure of outer control loop

Firstly, 3 phases load currents $\mathbf{i}_L = [i_{La}\ i_{Lb}\ i_{Lc}]^T$, 3 phases source voltages $v_s = [v_{sa}\ v_{sb}\ v_{sc}]^T$ are transformed to the $\alpha\beta$ frame by using the Clarke transformation with transitiosn matrix $\mathbf{F}$

$$\mathbf{v}_{s\alpha\beta} = \begin{bmatrix} v_{s\alpha} \\ v_{s\beta} \end{bmatrix} = \sqrt{\frac{2}{3}}\mathbf{F}\mathbf{v}_s,\ \mathbf{i}_{L\alpha\beta} = \begin{bmatrix} i_{L\alpha} \\ i_{L\beta} \end{bmatrix} = \sqrt{\frac{2}{3}}\mathbf{F}\mathbf{i}_L \text{ with } \mathbf{F} = \begin{bmatrix} 1 & -1/2 & -1/2 \\ 0 & \sqrt{3}/2 & -\sqrt{3}/2 \end{bmatrix} \quad (1)$$

We obtain the currents $i_{L\alpha}, i_{L\beta}$ and voltages $v_{s\alpha}, v_{s\beta}$ on the $\alpha\beta$ frame. Secondly, the currents and voltages on the $\alpha\beta$ frame are used to calculate the instantaneous active power and instantaneous reactive power that can be described in term of two parts: the low frequency and high frequencies as follow,

$$\begin{aligned} p &= v_{s\alpha} i_{L\alpha} + v_{s\beta} i_{L\beta} = \overline{p} + \tilde{p} \\ q &= v_{s\alpha} i_{L\beta} + v_{s\beta} i_{L\alpha} = \overline{q} + \tilde{q} \end{aligned} \quad (2)$$

in which $\overline{p}, \tilde{p}$ are the low frequency and the high frequency components of instantaneous active power, and $\overline{q}, \tilde{q}$ are the low frequency and the high frequency components of instantaneous reactive power. The instantaneous active power is passed through a low pass filter (LPF) to filter out the high frequency components $\tilde{p}$, the output of LPF is the $\overline{p}$. The compensation active power and reactive power are calculated by the equations as follow,

$$\begin{aligned} p_r &= \overline{p} - \left(\overline{p} + \tilde{p}\right) - p_{loss} = -\tilde{p} - p_{loss} \\ q_r &= \overline{q} + \tilde{q} \end{aligned} \quad (3)$$

The compensation currents on the $\alpha\beta$ $\mathbf{i}_{cref\alpha\beta} = [\, i_{cra} \quad i_{cr\beta} \,]^T$ are obtained by using the following relation:

$$\mathbf{i}_{cref\alpha\beta} = \frac{1}{v_{s\alpha}^2 + v_{s\beta}^2} \begin{bmatrix} v_{s\alpha} & -v_{s\beta} \\ v_{s\beta} & v_{s\alpha} \end{bmatrix} \begin{bmatrix} p_r \\ q_r \end{bmatrix} \quad (4)$$

The outer control loop calculating the equations (1)-(4) described as Figure 3 is implemented completely by the analog circuits that guarantes well the requirements of the transient time. The extra control loop using the PI controller has good performance. Recently, there are some methods developed to improve the responses of the outer control loop by focusing on the choice LPF's parameters [3]. The methods for turning better of the PI'parameters are presented on the materials [4, 5] by determining exactly the values *R*, V_{co} and *C* of SAF, by considering the offset of the parameters, by using the adaptive methods.

Beside, using the PI controller, the using neural networks **Error! Reference source not found.**, fuzzy technics [9] and wavelet [10] are developed recently to control the outer loop. To improves the performance of the outer control loop there are some turning PI controller's parameters, example the using of the optimal method PSO [11]. When consider the non-ideal mains voltage, in [12] presents the compensation engineering by using two LPFs for two source voltages on the *dq* frame. The inner loop's role is to control IGBT of SAF to generate the compensation currents injected to the power network such that it can track quickly the currents $i_{cr\alpha}, i_{cr\beta}$.

There are many methods to design inner loop's controller as PI control, known as fixed frequency control or hysteric current control [13]; the control engineering SFX-ADF [14, 15]; Delta modulation technic [16-18] or Dead-Bead [19, 20]. The control problem of inner control loop is most interesting research topics and this topic has attracted a great deal of attention from scholars to improve the dynamic characteristic, compensate completely the harmonics, reduce the THD, minimize the oscillation of power networks caused by nonlinear loads etc. Today, the applying neural network [21], fuzzy engineer control to the inner loop can improve the dynamic characteristic but implement hardly in practice due to the speed of microprocessor and calculation amount, so that so that this methods are currently theories [22-24].

The PI controllers have some advantages such as quickly response, easily setup and turning by analog circuits, however, the dynamics of the PI controller are inadequate because of the limited bandwidth of the controller. As a result, the SAF may not give the required performance when the loads have a high degree of non-linearity [5, 25].

This paper presents a control method for the inner loop of SAF by using the current model predictive on the *dq* frame. The method's advantage is that the transient period shorter than method using PI controller. The desired compensation currents can track exactly the reference compensation currents on the *dq* frame. The simulation results implemented on the nonlinear load, a full bridge rectifier and 3 phase unbalance load, show that the transient period decrease from 0.1s to 0.02s in comparing with PI controller. The experimental results proof that the THD of source currents decrease from 24.8% to 5.4% when using the proposed method. The rest of the paper is organized as follows: Section II describes the Controller design of inner loop for SAF based on current model prediction on *dq* frame. Section III illustrates simulation and experiment results. Finally, Section IV concludes the paper.

2. CONTROLLER DESIGN OF INNER LOOP FOR SAF BASED ON CURRENT MODEL PREDICTION ON *dq* FRAME

The control structure of the inner loop for SAF based on current model prediction on *dq* frame is shown in Figure 4.

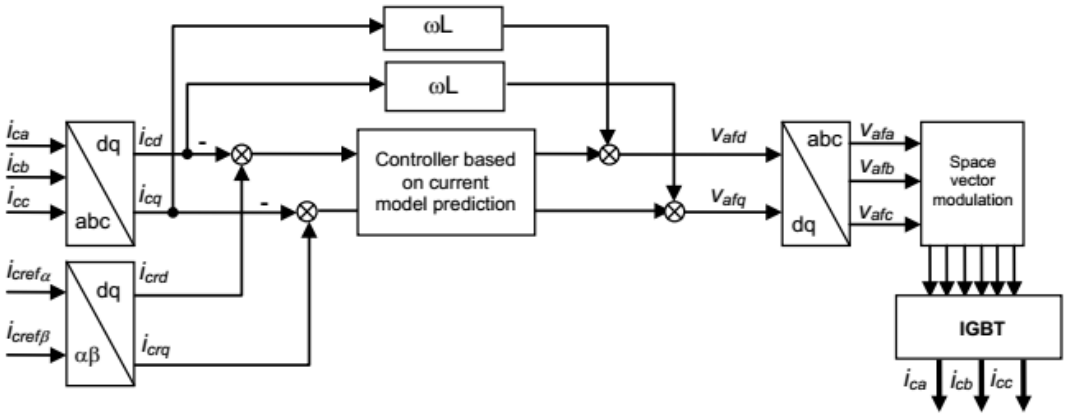

Figure 4. The control structure of SAF's inner loop based on current model prediction

To obtain the current model prediction for SAF, using the equations written on the *abc* frame by Kirchhoff II for SAF, with $\mathbf{v_{af}} = [\, v_{afa} \quad v_{afb} \quad v_{afc} \,]^T$ is voltage vector of SAF, we have:

$$\mathbf{v}_{\mathbf{af}} = R\mathbf{i}_{\mathbf{c}} + L\frac{d}{dt}\mathbf{i}_{\mathbf{c}} + \mathbf{v}_{\mathbf{s}} \tag{5}$$

where *R* and *L* are the output smoothing inductor inductance and resistance of the SAF. Transforming the equation (5) in synchronous reference frame using transformation matrix $\mathbf{G}$, we get the SAF voltages on the *dq* frame as,

$$\mathbf{v}_{\mathbf{sdq}} = \begin{bmatrix} v_{sd} & v_{sq} & v_{s0} \end{bmatrix}^T = \frac{2}{3}\mathbf{G}\mathbf{v}_{\mathbf{s}} \tag{6}$$

with $\mathbf{G}$ is defined on the material [26, 27]. The equation (5) is now written on the *dq* frame as,

$$\mathbf{v}_{\mathbf{afdq}} = R\mathbf{i}_{\mathbf{cdq}} + \omega L\begin{bmatrix} -i_{cq} \\ i_{cd} \\ i_{c0} \end{bmatrix} + L\frac{d}{dt}\mathbf{i}_{\mathbf{cdq}} + \mathbf{v}_{\mathbf{sdq}} \tag{7}$$

In order to obtain the current predictive model of SAF, discretizing equation (7) with sample time T_s, we have:

$$\mathbf{v}_{\mathbf{afdq}}(k) = R\mathbf{i}_{\mathbf{cdq}}(k) + \omega L\begin{bmatrix} -i_{cq}(k) \\ i_{cd}(k) \\ i_{c0}(k) \end{bmatrix} + \frac{L}{T_s}\left(\mathbf{i}_{\mathbf{cdq}}(k) - \mathbf{i}_{\mathbf{cdq}}(k-1)\right) + \mathbf{v}_{\mathbf{sdq}}(k) \tag{9}$$

The $\omega L[\, -i_{cq}(k) \quad i_{cd}(k) \quad i_{c0}(k) \,]^T$ is the cross coupling term between *d* and *q* axis. Assuming a three phase balanced power source, the $\mathbf{v}_{\mathbf{sdq}}(k)$ term can be removed, so the equation **Error! Reference source not found.** becomes

$$\mathbf{v}_{\mathbf{afdq}}(k) = \frac{RT_s + L}{T_s}\mathbf{i}_{\mathbf{cdq}}(k) + \omega L\begin{bmatrix} -i_{cq}(k) \\ i_{cd}(k) \\ i_{c0}(k) \end{bmatrix} - \frac{L}{T_s}\mathbf{i}_{\mathbf{cdq}}(k-1) \tag{10}$$

The current predictive model of the SAF at the time $k+1$ can be obtained by solving equation **Error! Reference source not found.** using the replacing $k = k+1$.

$$\mathbf{i}_{\mathbf{cdq}}(k+1) = \frac{T_s}{RT_s + L}\mathbf{v}_{\mathbf{afdq}}(k+1) - \frac{\omega L T_s}{RT_s + L}\begin{bmatrix} -i_{cq}(k+1) \\ i_{cd}(k+1) \\ i_{c0}(k+1) \end{bmatrix} + \frac{L}{RT_s + L}\mathbf{i}_{\mathbf{cdq}}(k) \tag{11}$$

When modeling the predictive controller, the feedback signal should take into account the drift in the predictive model equations due to the nonlinear nature of SAF, we consider the error between real output currents of SAF $\mathbf{i}_{\mathbf{cdqm}}(k)$ and predictive currents $\mathbf{i}_{\mathbf{cdq}}(k)$ calculated by model **Error! Reference source not found.** at the same discrete instance as $\mathbf{e}(k) = \mathbf{i}_{\mathbf{cdqm}}(k) - \mathbf{i}_{\mathbf{cdq}}(k)$. Therefore, an error $e(k)$ need to be added to the output predictive currents to correct, we have the corrected output predictive currents at next discrete instance as:

$$\hat{\mathbf{i}}_{\mathbf{cdq}}(k+1) = \mathbf{i}_{\mathbf{cdq}}(k+1) + \lambda \mathbf{e}(k) \tag{8}$$

where λ is the correction coefficient.

Next, use the objective function as:

$$J = \xi\left[\hat{\mathbf{i}}_{\mathbf{cdq}}(k+1) - \mathbf{i}_{\mathbf{crefdq}}(k+1)\right]^2 + \gamma \mathbf{v}_{\mathbf{afdq}}(k+1) \tag{9}$$

where ξ, γ are the weighting coefficient of the predictive error and the predictive control variable, respectively. It is noted that the control variable of SAF is voltages $\mathbf{v}_{\mathbf{afdq}}$. Substitution the $\mathbf{i}_{\mathbf{cdq}}(k+1)$ on the equation (11), we have:

$$\begin{aligned} J &= \xi\left[\hat{\mathbf{i}}_{\mathbf{cdq}}{}^2(k+1) - 2\hat{\mathbf{i}}_{\mathbf{cdq}}(k+1)\mathbf{i}_{\mathbf{crefdq}}(k+1) + \mathbf{i}_{\mathbf{crefdq}}{}^2(k+1)\right] + \gamma \mathbf{v}_{\mathbf{afdq}}(k+1) \\ &= \xi\left[\left(\mathbf{i}_{\mathbf{cdq}}(k+1) + \lambda \mathbf{e}(k)\right)^2 - 2\hat{\mathbf{i}}_{\mathbf{cdq}}(k+1)\mathbf{i}_{\mathbf{crefdq}}(k+1) + \mathbf{i}_{\mathbf{crefdq}}{}^2(k+1)\right] \\ &\quad + \gamma \mathbf{v}_{\mathbf{afdq}}(k+1) \end{aligned} \tag{10}$$

The optimal control variable can be obtained by differentiating the object function J with respect to the voltage and equating that to zero $dJ/dt = 0$, the optimal control voltage variable can be found to be:

$$\mathbf{v}_{\mathbf{afdq}}(k+1) = \frac{T_s\xi\left(RT_s + L\right)}{\gamma\left(RT_s + L\right)^2 + T_s{}^2\xi}\left(\mathbf{i}_{\mathbf{crefdq}}(k+1) - \frac{L}{RT_s + L}\mathbf{i}_{\mathbf{cdq}}(k) - \mathbf{e}(k)\right) \tag{11}$$

The block diagram of the optimal control voltage variable for simulation and practical implementation is shown in Figure 5.

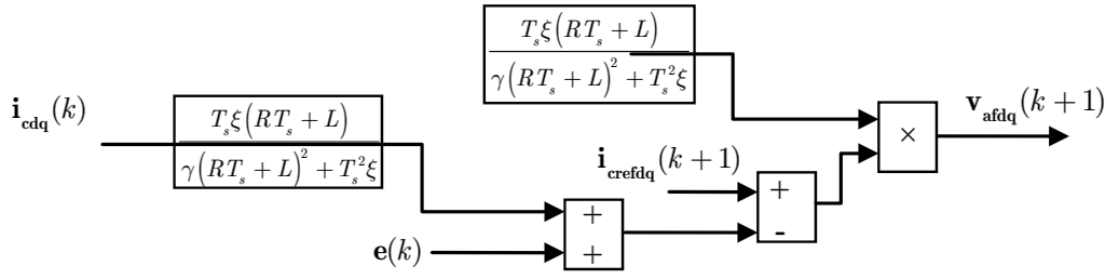

Figure 5. The diagram for inner controller of SAF based on current predictive model

The control law for the inner control loop of SAF established by equation (11) has the simple structure, the control action for the next discrete instance is the control voltage sending to the space vector modulation block to drive IGBT bridge generating the desired compensation currents.

The control law (11) take into account the predictive compensation currents on the discrete instance $k+1$, $\mathbf{i}_{\mathbf{cdq}}(k+1)$, in order to get the demand such as the error between the output predictive current of SAF and SAF's desired output current $\mathbf{i}_{\mathbf{crefdq}}(k+1)$ is minimize at the next discrete instance, so J reach to minimum. The cost function J includes two terms: the output current error $\hat{\mathbf{i}}_{\mathbf{cdq}}(k+1)-\mathbf{i}_{\mathbf{crefdq}}(k+1)$ and control voltage $\mathbf{v}_{\mathbf{afdq}}(k+1)$ with two adjustment parameters ξ and γ.

3. THE SIMULATION AND EXPERIMENTAL RESULTS

The simulation parameters: The nonlinear load consist of two loads connected in parallel: the full bridge rectifier supplying voltage for the DC load with $R_t = 10\Omega$, and the 3 phase unbalanced load with $R_{LA} = 2\Omega, R_{LB} = 4\Omega, R_{LC} = 6\Omega$. The resistance and inductance of load wire is $R_{Lr} = 0.001\Omega, L_{Lr} = 1e-6H$, respectively. Three phase voltage source has $U_d = 380V, f = 50Hz$, the source resistance and source inductance are $R_{Ln} = 0.001\Omega, L_{Ln} = 1e-8H$. The resistance and inductance of the wire from source to load are respectively $R_{gl} = 0.001\Omega, L_{gl} = 1e-6H$. The SAF has IGBT with snubber resistance $R_s = 10000\Omega,$, snubber capacitance $C_s = \infty(F),$ the ON resistance $R_{on} = 10^{-4}\Omega$, the forward voltages are 1 V, $T_f = 10^{-6}s, T_t = 2\times10^{-6}s$. The smooth inductance is $L_{ck} = 1.2\times10^{-3}H$. The extra PI controller has $K_p = 0.1; K_i = 1$, $U_{dc} = 1000V$. The sample time is $T_s = 5e-6H,$ the ode45 (dormand-Prince) is used to solve the discrete differential equations. The simulation results are shown in Figure 6 to 16. The Figure 6 shows the source voltage, Figure 7 represents the load currents or source currents in the case not using SAF. The Figure 8 illustrates the source currents when using SAF. The Figure 9 demonstrates the compensation currents determined by the outer control loop and the real compensation currents made by inner loop to inject to the network, which caused by the control law (11). The Figure 10 and Figure 11 depict the harmonic analysis of the source and load currents when using SAF. The Figure 12 introduced the varying of the voltage across capacitor. The desired compensation currents and real currents on the d frame are figured out in the Figure 13, the control voltage of SAF on the d frame is painted in the Figure 14. The Figure 15 and Figure 16 show the space modulation control voltage on the *abc* frame and IGBT control voltages, respectively.

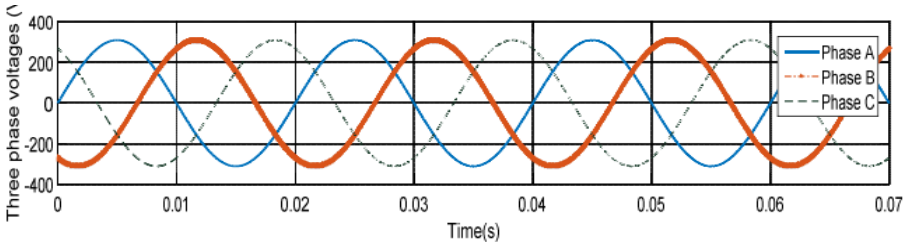

Figure 6. The 3 phase source voltages

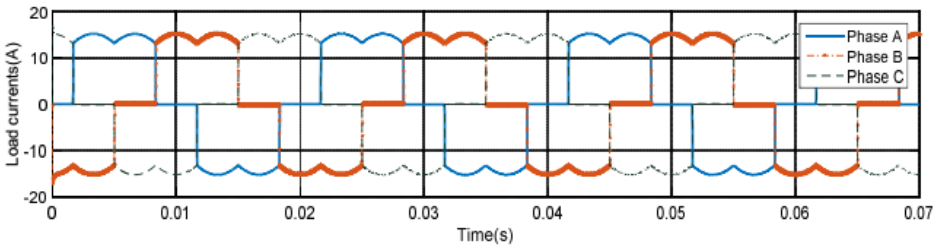

Figure 7. The load currents or source currents in the case not using SAF

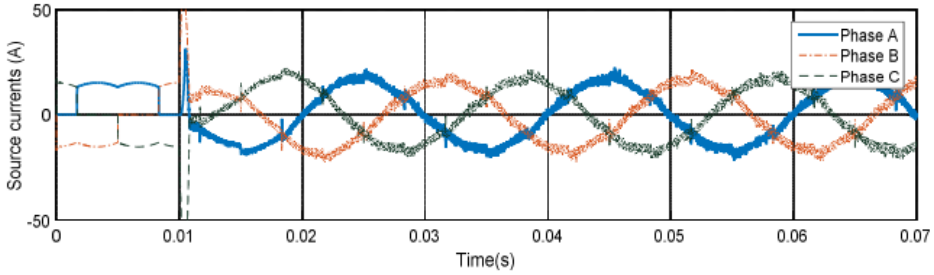

Figure 8. The source currents when using SAF

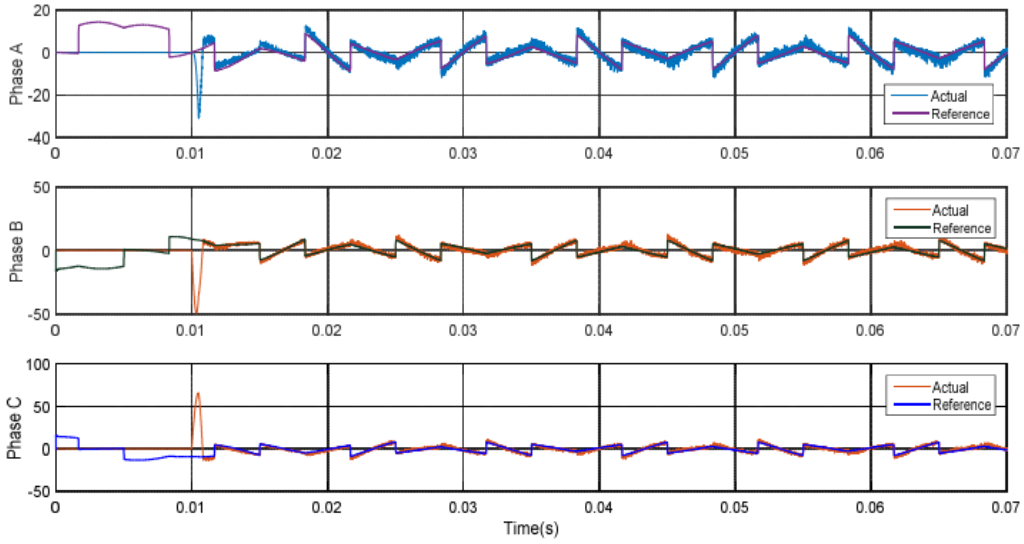

Figure 9. The compensation currents determined by the outer control loop and the real compensation currents made by inner loop to inject to the network

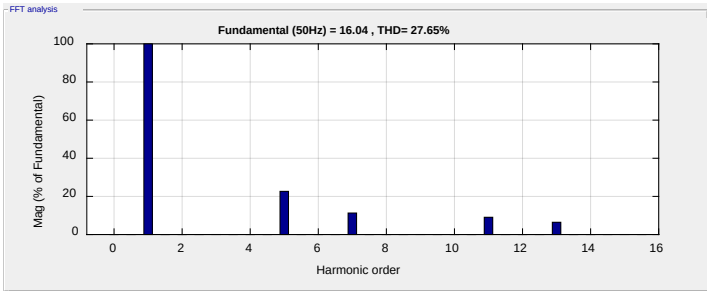

Figure 10. The harmonic analysis of the load currents

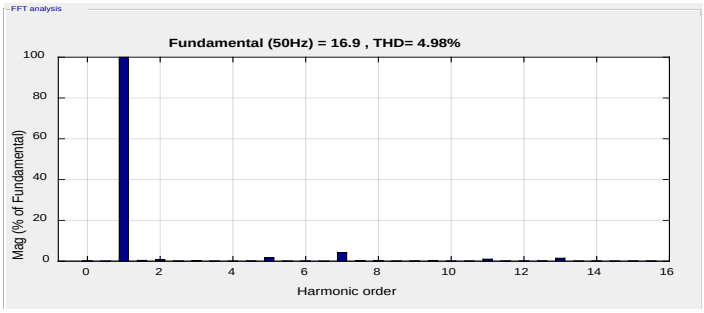

Figure 11. The harmonic analysis of the source when using SAF

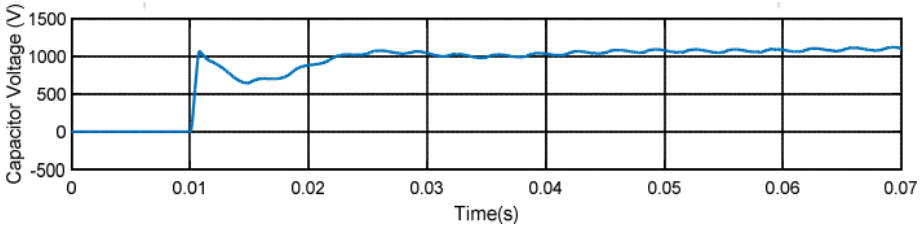

Figure 12. The varying of the voltage across capacitor of the SAF

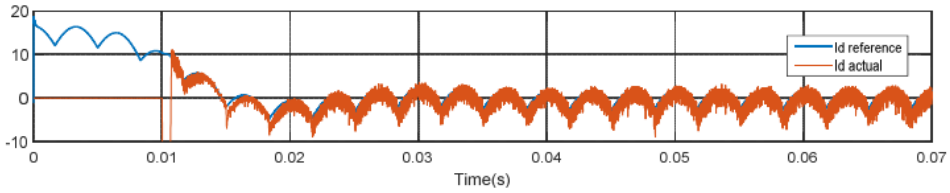

Figure 13. The desired compensation currents and real currents on the d frame

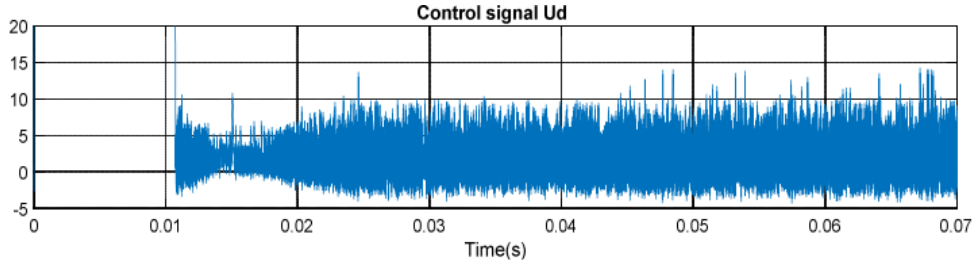

Figure 14. The control voltage of SAF on the d frame

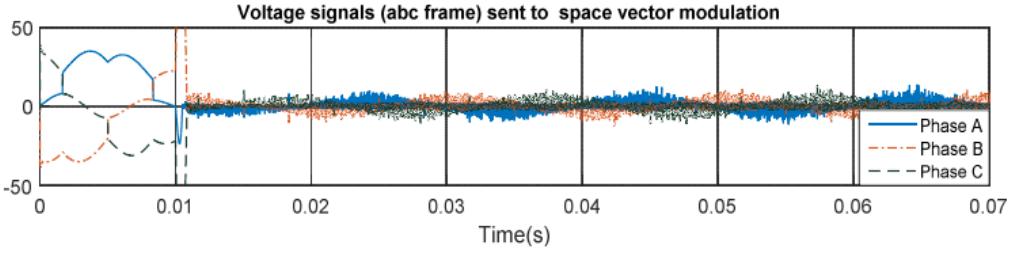

Figure 15. The space modulation control voltage on the *abc* frame

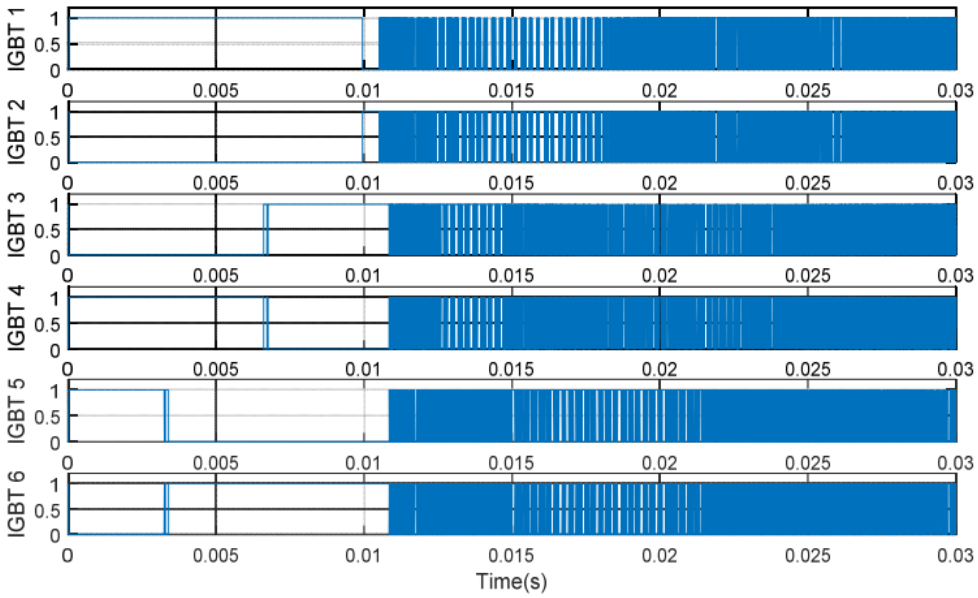

Figure 16. The IGBT control voltages

When not using the SAF to filter the harmonics, the harmonic current distortion are affected by the nonlinear loads (see Figure 7) with THD is 27.65%, in which the 5th order harmonic is 22%, the 7th order harmonic is 10%, the 10th , 11th, 13th order harmonics are 22%, when connecting the SAF to the network, the THD of the source currents decrease rapidly to 4.98%, the fundamental current component (50Hz) is approximately 100%, the 3, 5, 9, 11, 13th order harmonics are not reached to 1%, the 7th harmonics is 3%.

The advantage of the control law (11) is represented on the Figure 9, the real compensation currents on the phases A, B, C track completely to the desired compensation currents by transient time 0.012s. The real compensation current on the d axis is illustrated in the Figure 10. The transient period is shorter appreciably in comparing with using the PI controller in the materials [28, 29] which is 0.1s. The Table 1 demonstrates the THD varying of the source currents by changing the load. THD has upward trend when the load power is decrease and vice versa. If R_t is 10Ω then THD is 4.98%, however if R_t is 25Ω then THD is increasingly 4.98%. The experimental result is shown in the Figure 17.

Table 1. Comparing the varying of THD by the changing of the load

3Ω	4Ω	6Ω	8Ω	10Ω	15Ω	20Ω	25Ω
24.05%	24.32%	25.21%	25.74%	27.65%	27.84%	27.84%	28.26%
4.51%	4.53%	4.61%	4.77%	4.98%	5.01%	5.07%	5.11%

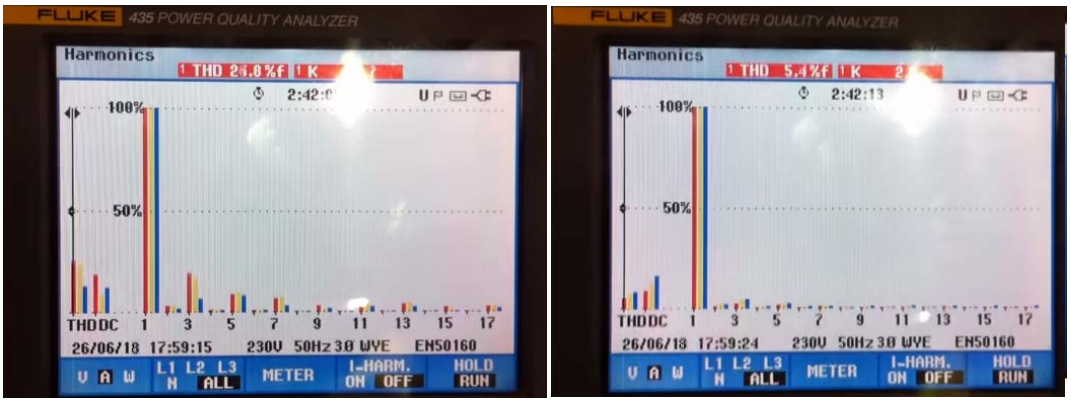

Figure 17. The experimental results

After asemblying completely the SAF electronic circuit, it is tested and we get the results as representing in the Figure 12. The harmonic analysics results show that before and after connecting the SAF to the network, THD of the source current is 24.8% and 5.4%, respectively. This result illustrate initially that the SAF electronic circuit implemented properly the SAF's function. There is slightly difference between the simulation and experimental results that is caused by the instrument turning, curcuit's parameters not to be chosen properly, the parameters's drift. The authors will continuely modify and complete in the future works.

4. CONCLUSION

The paper deals with the method for control output currents of SAF based on the *dq* frame using the SAF's current predictive model, the control action is derived by minimizing the cost function related to two term which are the error between the SAF's predictive currents $\hat{\mathbf{i}}_{\mathbf{cdq}}(k+1)$ and output desired currents $\mathbf{i}_{\mathbf{crefdq}}(k+1)$ in the next sample time, and the control voltages $\mathbf{v}_{\mathbf{afdq}}(k+1)$. The form of the control law is quietly simple and easily implement by analog circuits. The simulation and experimentation conducted by using the nonlinear load including the full bridge rectifier and 3 phase unbalance load show that the quality of the harmonic compensation meets the requirements of the IEE std 519. The THD of the source currents decrease quickly from 27.65% to 4.98% for simulation and 26.8% to 5.4% for experimentation. The fundamental current component (50Hz) is approximately 100%, the 3, 5, 9, 11, 13th order harmonics are not reached to 1%, the 7th harmonics is 3%. After transient period 0.012s, the SAF's output real compensation currents track completely the desired compensation currents required by outer loop. The transient period gets faster than method using the PI controller in [28, 29].

REFERENCES

[1] Jian Dai, Minghao Wen, Ertao Lei, Yu Chen, Haihuan Wu, and Xianggen Yin, "A Comprehensive Control Strategy Suitable for Reactive Power Compensation and Harmonic Elimination," 12th *World Congress on Intelligent Control and Automation (WCICA)*, June 12-15, 2016, Guilin, China.

[2] R. Zahiraa and A. Peer Fathima, "A Technical Survey on Control Strategies of Active Filter for Harmonic Suppression," *International Conference on Communication Technology and System Design 2011, Procedia Engineering 30*, pp. 686 – 693, 2012.

[3] A. Boukadoum and T. Bahi, "Fuzzy Logic Controlled Shunt Active Power Filter for Harmonic Compensation and Power Quality Improvement," *Journal of Engineering Science and Technology Review*, vol. 7(4), pp. 143-149, 2014.

[4] R. B. Yamarthi, R. S. Rao, and P. L. Reddy, "Effect of PI Controller Parameters on the Performance of Shunt Active Power Filter," *International Research Journal of Engineering and Technology*, vol. 3, issue: 10, oct 2016.

[5] Simone Buso, Luigi Malesani, and Paolo Mattavelli, "Comparison of Current Control Techniques for Active Filter Applications," *IEEE transactions on industrial electronics*, vol. 45, no. 5, october 1998.

[6] Xingang Fu and Shuhui Li, "A Novel Neural Network Vector Control for Single-Phase Grid-Connected Converters with L, LC and LCL Filters," *Energies*, vol. 9(5), pp. 328, 2016.

[7] Yu Dongmei, Guo Qingding, Hu Qing, and Liu chunfang, "A Novel DSP Based Current Controller with Fuzzy Variable-Band hysteresis for Active Power Filters," *Transmission and Distribution Conference and Exhibition: Asia and Pacific, IEEE/PES*, 2005.

[8] Nixuan Liu and Juntao Fei, "Adaptive Fractional Sliding Mode Control of Active Power Filter Based on Dual RBF Neural Networks," *IEEE Access*, vol. 5, 2017.

[9] D. A Gadanayak and P. C. Panda, "A Novel Fuzzy Variable Band Hysteresis Current Controller for Shunt Acticve Power Filters," *ACEEE Int. J. con Control System and Instrumentation*, vol. 2, no. (2), June 2011.

[10] Malabika Basu and Biswajit Basu, "A Wavelet Controller for Shunt Active Power Filter," *3rd IET International Conference on Power Electronics, Machines and Drives*, Dublin, Ireland, pp.76-79, 2006.

[11] Shubhendra Yadav, Vipin Kumar Singh, and Satyendra Singh, "Particle Swarm Optimization Based Shunt Active," *4th IEEE Uttar Pradesh Section International Conference on Electrical, Computer and Electronics (UPCON)* GLA University, Mathura, Oct 26-28, 2017.

[12] Murat Kale and Engin Ozdemir, "Harmonic and Reactive Power Compensation with Shunt Active, Power Filter Under Non-Ideal Mains Voltage," *Electric Power Systems Research*, vol. 74, pp. 363–370, 2005.

[13] R. Arun; B. Ramkiran, and Ayyapan, "Shunt Active Power Filter using Hysteresis and PI control for Improving the Power Quality using MATLAB," *Green Engineering and Technologies (IC-GET), 2015 Online International Conference on Green Engineering and Technologies* (IC-GET), 27-27 Nov. IEEE 2015.

[14] S. Fukuda, T. Kanayama, and K. Muraoka, "SFX Algorithm Based Adaptive Control of Active Filters without Detecting Current Harmonics," *IEEE 2004*.

[15] S. Fukuda, K. Muraoka, and T. Kanayama, "Adaptive Learning Based Current Control of Active Filters Needless to Detect Current Harmonics," *Applied Power Electronics Conference and Exposition, 2004, APEC '04, Nineteenth Annual IEEE*, Vol. 1, pp. 210–216, 2004.

[16] E. Wiebe-Quintana,"Delta-Sigma Integral Sliding-Mode Control Strategy of a Three-Phase Active Power Filter using d-q Frame Theory," *Proceedings of the Electronics, Robotics and Automotive Mechanics Conference (CERMA'06) IEEE computer society*, 2006.
[17] R. Kazemzadeh; J. Amini; and E. Najafi Aghdam," Sigma-Delta Modulation Applied to a 3-Phase Shunt Active Power Filter using Compensation with Instantaneous Power Theory," *The 2nd International Conference on Computer and Automation Engineering (ICCAE)*, vol. 5, pp. 88–92, 2010.
[18] A. Jeraldine Viji; R. Pushpalatha; M. Rekha, "Comparison of a Active Harmonic Compensator with PWM and Delta Modulation Under Distorted Voltage Conditions," *international Conference on Recent Advancements in Electrical, Electronics and Control Engineering*, pp. 82–86, 2011.
[19] R. Panigrahi; P. C. Panda; and B. D. Subudhi, "Comparison of Performances of Hysteresis and Dead Beat Controllers in Active Power Filtering," *IEEE Third International Conference on Sustainable Energy Technologies (ICSET)*, pp. 287-292, 2012.
[20] C. Wang, Z. Zhou, Y. Liu, M. S. Kanniche, P. M. Holland, R. P. Lewis, S. G. Batcup, and P. Igic, "A Predictive Dead-Beat PI Current Controller for Active Power Filters," *Proceedings of the 2011 14th European Conference on Power Electronics and Applications*, pp: 1–8, 2011.
[21] M. A. M. Radzi and N. A. Rahim, "Neural Network and Bandless Hysteresis Approach to Control Switched Capacitor Active Power Filter for Reduction of Harmonics," *IEEE Trans. Industr. Electron.*, vol. 56, no. 5, pp. 1477-1484, May 2009.
[22] X. G. Fu, S. H. Li, M. Fairbank, D. C. Wunsch, and E. Alonso, "Training Recurrent Neural Networks with the Levenberg-Marquardt Algorithm for Optimal Control of a Grid-Connected Converter," *IEEE Trans. Neural Netw. Learn. Syst.*, vol. 26, no. 9, pp. 1900-1912, Sep. 2015.
[23] R. P. Aguilera, P. Acuna, P. Lezana, G. Konstantinou, B. Wu, S. Bernet, and V. G. Agelidis, "Selective Harmonic Elimination Model Predictive Control for Multilevel Power Converters," *IEEE Trans. Power Electron.*, vol. 32, no. 3, pp. 2416-2426, March 2017.
[24] P. Karuppanan and Kamalakanta Mahapatra, "Active Harmonic Current Compensation to Enhance Power Quality," *Electrical Power and Energy Systems*, vol. 62, pp. 144–151, 2014.
[25] W. T. Guo, F. Liu, J. Si, D. W. He, R. Harley, and S. W. Mei, "Online Supplementary ADP Learning Controller Design and Application to Power System Frequency Control with Large-Scale Wind Energy Integration," *IEEE Trans. Neural Netw. Lear. Syst.*, vol. 27, no. 8, pp. 1748-1761, 2016.
[26] Luca Tarisciotti, Andrea Formentini, Alberto Gaeta, Marco Degano, Pericle Zanchetta, Roberto Rabbeni, and Marcello Pucci, "Model Predictive Control for Shunt Active Filters with Fixed Switching Frequency," *IEEE transactions on industry applications*, vol. 53, no. 1, January/February 2017.
[27] Chao Meng, Lin Zhang, Yongqiang Hong, and Junbin Lin, "A Novel Control Strategy for Three-Phase Shunt Active Power Filter using a Lyapunov Function," *Proceedings of the 7th International Power Electronics and Motion Control Conference, IEEE*, 06 August 2012
[28] Consalva J. Msigwa, Beda J. Kundy, and Bakari M.M. Mwinyiwiwa, "Control Algorithm for Shunt Active Power Filter using Synchronous Reference Frame Theory," *World Academy of Science, Engineering and Technology International Journal of Electrical and Computer Engineering*, vol. 3, no. 10, 2009.
[29] M. T. Benchouiaa, I. Ghadbanea, A. Goleaa, K. Srairib, and M. H. Benbouzidc, "Design and Implementation of Sliding Mode and PI Controllers based Control for Three Phase Shunt Active Power Filter," *The International Conference on Technologies and Materials for Renewable Energy, Environment and Sustainability, TMREES14, Science Direct, Energy Procedia*, vol. 50, pp. 504–511, 2014.